九州大学大学院総合理工学報告
第 47 巻 第 1 号 17-23 頁 令和 7 年 9 月

Engineering Sciences Reports, Kyushu University
Vol. 47, No. 1, pp. 17-23, SEP, 2025

Photochemical Removal of Acrolein Using a Head-on Type of 172-nm Xe_2 Excimer Lamp in Air at Atmospheric pressure

Masaharu TSUJI,[*1,2†] Naohiro KAMO[*3] and Masato MIYANO[*3]
[†]E-mail of corresponding author: tsuji@cm.kyushu-u.ac.jp

(Received Aug 18, 2025, accepted Aug 30, 2025)

The photochemical removal of acrolein (C_2H_3CHO) was investigated in air (O_2 5–20%) at atmospheric pressure using a head-on type of 172-nm Xe_2 excimer lamp. When 172-nm light was irradiated to C_2H_3CHO, HCHO, HCOOH, CO, CO_2, and O_3 were observed in FTIR spectra. The dependence of product concentrations on the irradiation time indicated that C_2H_3CHO is converted to CO_2 via HCHO, HCOOH, and CO intermediates. The initial removal rates of C_2H_3CHO increased from 0.80 to 1.43 min^{-1} with decreasing the O_2 concentration from 20 to 5%. Besides direct photolysis of C_2H_3CHO, $O(^3P)$, $O(^1D)$, and O_3 are possible active species of C_2H_3CHO removal. The contribution of $O(^1D)$ was examined from the total pressure dependence of the residual amount of C_2H_3CHO, and that of O_3 was obtained from the O_3 + C_2H_3CHO reaction in the same apparatus. It was inferred that C_2H_3CHO is initially decomposed by direct vacuum ultraviolet (VUV) photolysis of C_2H_3CHO and the $O(^3P)$ + C_2H_3CHO reaction. It was oxidized further by reactions of H, $O(^3P,^1D)$, OH, and O_3 with various intermediates such as HCHO, HCOOH, and CO, leading to CO_2 as a final product.

Key words: *VOC, Acrolein, Oxidation, VUV photolysis, Head-on type of 172 nm Xe_2 excimer lamp, $O(^3P)$, $O(^1D)$, O_3, CO, CO_2*

1. Introduction

Volatile organic compounds (VOCs) are emitted as gases from certain solids or liquids. VOCs include a variety of chemicals, some of which may have short- and long-term adverse health effects. Current removal techniques of VOCs are thermal oxidation, adsorption, biofiltration, non-thermal plasma, photodegradation, catalysts, and photocatalysis.[1-7] Removal of VOCs by using VUV photons is a new promising technique. In discharge plasmas in air, where energetic electrons are major active species, N_2 molecules are decomposed, and active N atoms are formed. Therefore, toxic NOx molecules are generated through the N + O_2 and NO + O_3 reactions during removal of VOCs. An advantage of 172-nm VUV photolysis in air is that N_2 molecules are not decomposed, so that no NOx molecules are formed during photolysis. We have studied removal of such typical VOCs as CH_4, C_2H_4, and aldehydes using head-on and/or side-on types of 172-nm VUV excimer lamps.[8-14] Results demonstrated that these VOC can be removed efficiently in air at atmospheric pressure and at low temperatures without using any catalysts.

Acrolein (C_2H_3CHO) is a highly toxic VOC which should be removed efficiently. In this study, 172-nm VUV photolysis of acrolein in air is studied using a head-on type of 172-nm excimer lamp. Removal rates of C_2H_3CHO in air are measured at 20, 10, or 5% O_2. Results obtained are compared with our previous data obtained using a side-on type of 172-nm excimer lamp.[11]

In 172-nm photolysis in air, ground state $O(^3P)$ atoms and metastable $O(^1D)$ atoms are formed by photolysis of O_2.[15,16] O_3 molecules are formed by the subsequent three-body $O(^3P)$ + O_2 + N_2 (or O_2) reactions. Therefore, in addition to direct VUV photodissociation, reactions of $O(^3P,^1D)$ and O_3 with C_2H_3CHO might be responsible for C_2H_3CHO removal in the initial decomposition reactions. The contribution of $O(^1D)$ is examined by measuring the dependence of the residual amount on the total pressure. To examine the contribution of

*1 Institute for Materials Chemistry and Engineering, and Research and Education Center of Green Technology
*2 Department of Applied Science for Electronics and Materials
*3 Department of Applied Science for Electronics and Materials, Graduate Student

O_3, the O_3 + C_2H_3CHO reaction is studied using the same apparatus. Based on these experiments, major active species under 172-nm photolysis of C_2H_3CHO are determined and the oxidation mechanism of C_2H_3CHO is discussed. All reaction rate constants and branching ratios of products used for discussion have been measured at about 300 K.[17]

2. Experimental

The VUV photolysis apparatus used in this work was the same as that reported previously.[9,10] We used a head-on type of 172-nm excimer lamp with an input power of 20 W. Light from an unfocused 172-nm Xe_2 lamp (50 mW/cm^2, 155–200 nm range, UER20H172; Ushio Inc.) was irradiated into the photolysis chamber through a quartz window. Experiments were conducted using a closed batch chamber at atmospheric pressure with a chamber volume of 184 mL. The C_2H_3CHO concentration diluted in N_2/O_2 mixtures (20, 10, or 5% O_2) was 500 ppm in most experiments. Product gases in the photolysis chamber were analyzed using a gas analysis system (FG122-LS; Horiba Ltd.) equipped with a Fourier transform infrared (FTIR) spectrometer. The spectra in the 800–4000 cm^{-1} region were monitored. The CO, CO_2, HCHO, and C_2H_3CHO concentrations were calibrated using standard gases. On the other hand, the O_3 and HCOOH concentrations were evaluated by reference to standard spectral data supplied by Horiba Ltd.

We have also studied the O_3 + C_2H_3CHO reaction using the same technique reported previously.[10] The initial C_2H_3CHO, O_2, and O_3 concentrations in a C_2H_3CHO /air mixture were 260 ppm, 20%, and 0.69%, respectively. The total pressure was 50 kPa.

We used the following gases: N_2 (purity >99.9998%; Taiyo Nippon Sanso (TNS) Corp.), O_2 (purity >99.99995%; TNS Corp.), and C_2H_3CHO (4800 ppm in N_2 buffer gas; TNS Corp.). C_2H_3CHO was diluted in air (5, 10, or 20%) before use.

3. Results and discussion

3.1 C_2H_3CHO removal by 172-nm VUV phtons in air at 20, 10, or 5% O_2

The 172-nm photolysis of C_2H_3CHO in air was conducted at 20, 10, or 5% O_2. As an example, Fig. 1(a) shows a typical FTIR spectrum of C_2H_3CHO (500 ppm) at 20% O_2 before photoirradiation, where a strong C_2H_3CHO peak at about 1730 cm^{-1} and a few weak C_2H_3CHO peaks are observed in the 1100–2800 cm^{-1} region. FTIR spectra at 10 or 5% O_2 before photoirradiation were essentially identical with Fig. 1(a). Figures 1(b)–1(d) show FTIR spectra obtained after photoirradiation for 1 min at 20, 10, or 5% O_2, respectively. After

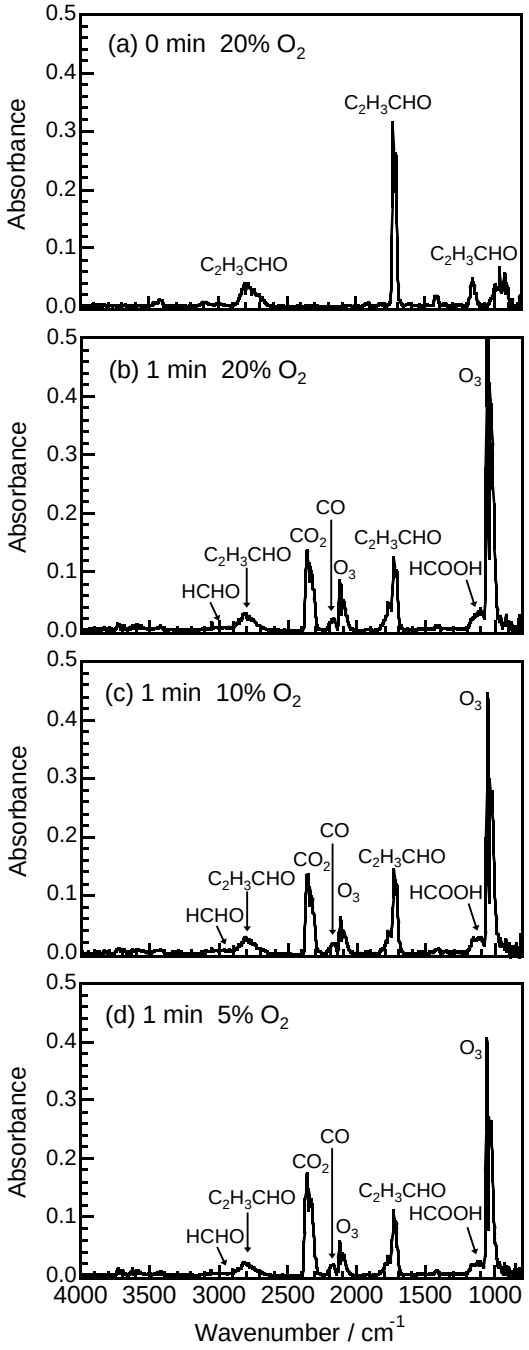

Fig. 1. (a) FTIR spectra of C_2H_3CHO and products (a) before 172-nm photoirradiation in 20% O_2 and (b)–(d) after photoirradiation for 1 min at 20% O_2, 10% O_2, and 5% O_2, respectively.

photolysis for 1 min, the C_2H_3CHO peaks decrease their intensities by 54–77%, whereas CO, CO_2, HCHO, HCOOH, and O_3 peaks appear. The concentration of O_3 decreases with decreasing the O_2 concentration.

Figures 2(a)–2(c) show the dependence of the concentrations of C_2H_3CHO, HCHO, HCOOH, CO, CO_2, and O_3 on the irradiation time at O_2 concentrations of 20, 10, and 5%, respectively. Results show that the concentration C_2H_3CHO rapidly decreases to zero at about 5 min in all cases. Time profiles of the concentrations of HCHO, HCOOH, and CO at 20 and 10% O_2 are similar and give peaks at 1.5, 3.5, and 2.5 min, respectively. The concentrations of HCHO, HCOOH, and CO at 5% O_2 give peaks at 2.0, 2.5, and 2.5 min, respectively. The concentration of CO_2 increases to about 285 ppm at 20 min in all cases. The concentration of O_3 increases to 1.29, 0.80, and 0.48% at 20, 10, and 5% O_2, respectively, after 20 min irradiation. These time profiles imply that C_2H_3CHO is finally converted to CO_2 via HCHO, HCOOH and CO through consecutive reactions.

Assuming pseudo-first order decay, the initial C_2H_3CHO removal rate constants k_p were ascertained from slopes of $-\ln(C_t/C_0)$ vs. irradiation time, where C_0 is the initial concentration of C_2H_3CHO. The k_p values were 0.80, 0.87, and 1.43 min^{-1} at the O_2 concentration of 20, 10, and 5%, respectively. These values were smaller than those obtained using a side-on lamp by factors of 10.5, 13.4, and 11.6, respectively.[11] A major reason for the small removal rates is that the window area of the head-on lamp (8.0 cm^2) was smaller than that of the side-on type one (78.5 cm^2) by about one order of magnitude.[9,10] Therefore, reaction volume in the head-on lamp experiments is about one order of magnitude smaller than that in the side-on ones.

With decreasing the O_2 concentration from 20% to 10, and 5%, the light transmittance distance above 95% increases, respectively, from ≈1 cm to ≈2, and ≈4 cm.[9,10] Therefore, the reaction volume increases concomitantly with decreasing the O_2 concentration because the VUV light penetrates into the reaction chamber with decreasing the O_2 concentration. VUV photolysis of O_2 and C_2H_3CHO occur in a large reaction volume uniformly with decreasing the O_2 concentration. This uniformity is a major reason why the C_2H_3CHO removal rate increases concomitantly with decreasing the O_2 concentration.

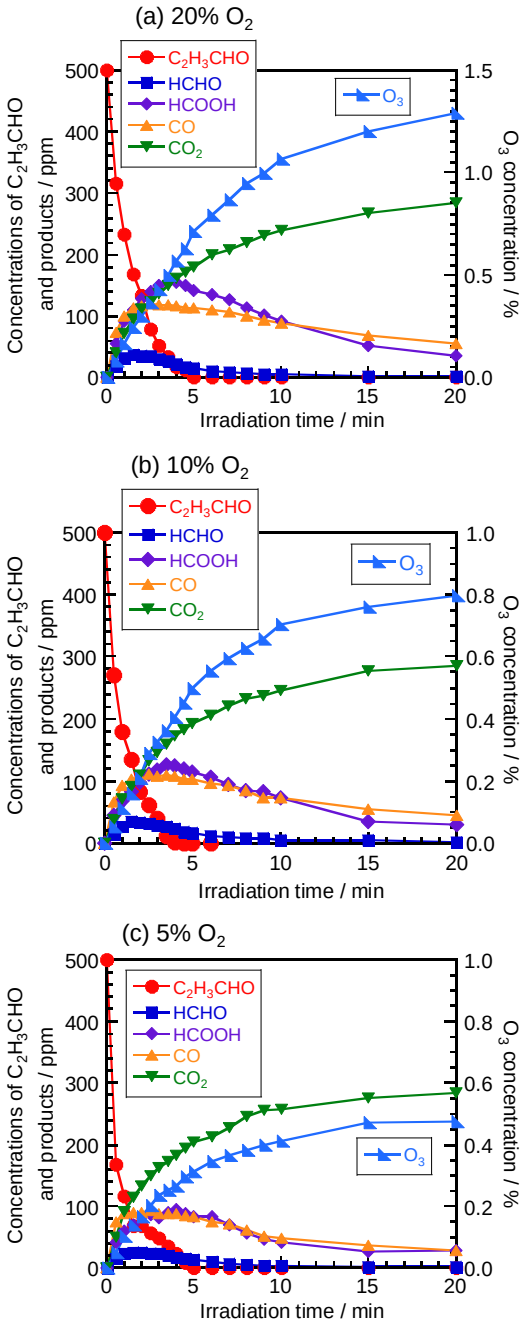

Fig. 2. Dependence of concentrations of C_2H_3CHO, products, and O_3 on the irradiation time at (a) 20% O_2, (b) 10% O_2, and (c) 5% O_2.

3.2 Effects of O(¹D) atoms in C_2H_3CHO removal

The effect of O(¹D) was examined by changing the total operating pressure of the reaction chamber. O(¹D) atoms are formed by 172-nm photolysis of O_2 (1).[16] The O(¹D) + C_2H_3CHO reaction (3) competes with the quenching reactions by N_2 (3) and O_2 (4).

$O_2 + h\nu(172\text{-nm}) \rightarrow O(^3P) + O(^1D)$ (1)

$O(^3P) + C_2H_3CHO \rightarrow$ Products (2)

($k_2 = 4.01 \times 10^{-13}$ cm^3 molecule^{-1} s^{-1})[17]

$O(^1D) + C_2H_3CHO \rightarrow$ Products (3)

$O(^1D) + N_2 \rightarrow O(^3P) + N_2$ (4)

($k_4 = 2.6 \times 10^{-11}$ cm^3 molecule^{-1} s^{-1})[17]

$O(^1D) + O_2 \rightarrow O(^3P) + O_2$ (5)

($k_5 = 4.0 \times 10^{-11}$ cm^3 molecule^{-1} s^{-1})[17]

Although the rate constant of the $O(^3P)$ + C_2H_3CHO reaction (2) has been reported, that of the $O(^1D)$ + C_2H_3CHO reaction (3) has not been measured. With decreasing the total pressure, the relative contribution of process (3) to those of (4) and (5) increases because electronic quenching reactions (4) and (5) are suppressed at low N_2/O_2 pressures.

Figure 3 presents the dependence of the residual amount of C_2H_3CHO defined by C_t/C_0 and the concentration of O_3 on the total pressure of air (20% O_2) after 1 min photoirradiation. If the $O(^1D)$ + C_2H_3CHO reaction (3) plays a major role in the C_2H_3CHO removal as in the case of the $O(^1D)$ + CH_4 reaction,[12] the residual amount of C_2H_3CHO is expected to decrease with decreasing the total pressure. No significant decrease in the residual amount of C_2H_3CHO is found with decreasing the total pressure from 100 to 10 kPa, indicating that $O(^1D)$ atoms play no major role for the C_2H_3CHO removal. The O_3 concentration decreases from 0.14 to 0.0064% with decreasing the total pressure from 100 to 10 kPa because three-body $O(^3P) + O_2 + X$ (X = N_2, O_2) reactions leading to O_3 are suppressed with decreasing the total pressure. Results

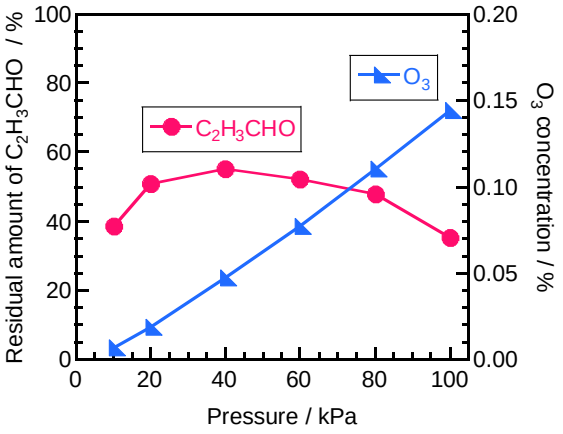

Fig. 3. Dependence of residual amount of C_2H_3CHO and the concentration of O_3 on the total pressure of air (20% O_2) after 1 min photoirradiation. The initial concentration of

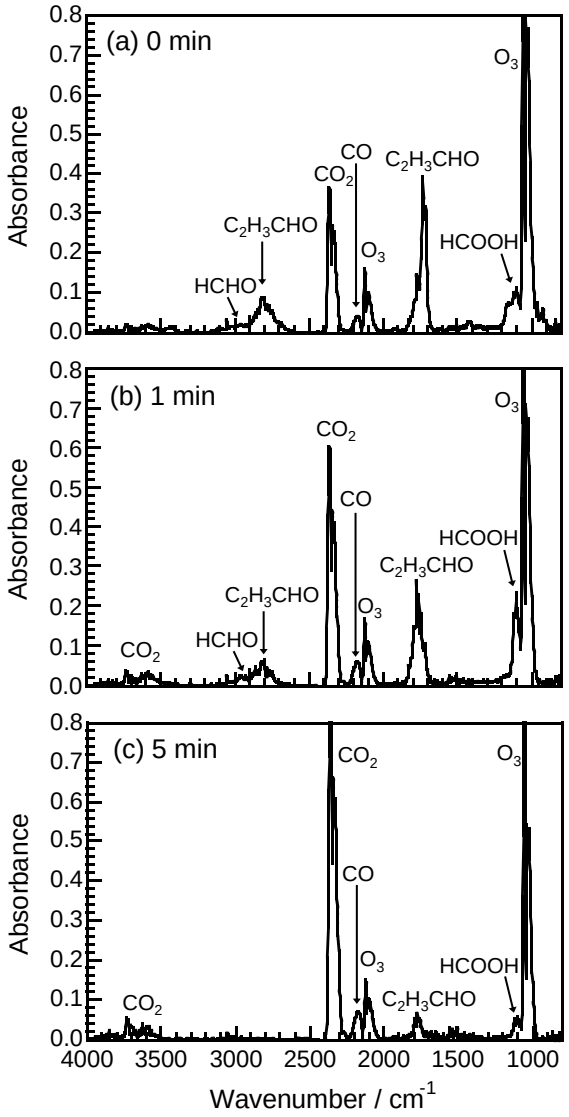

Fig. 4. (a) FTIR spectra of C_2H_3CHO and products by the O_3 + C_2H_3CHO reaction at reaction times of 0, 1, and 5 min, respectively.

demonstrate that the residual amount of C_2H_3CHO after 1 min photoirradiation is essentially independent of the O_3 concentration. This implies that O_3 molecules are not major active species in the initial stage below 1 min.

3.3 Effects of O_3 on C_2H_3CHO removal

To confirm the contribution of O_3 for the C_2H_3CHO removal, the O_3 + C_2H_3CHO reaction was studied at an initial O_3 concentration of 0.69%. Figures 4 respectively depict FTIR spectra of C_2H_3CHO obtained from the O_3 + C_2H_3CHO reaction at reaction times of 0, 1, and 5 min, respectively, where HCHO, HCOOH, CO, CO_2, and O_3 peaks are observed. The reaction starts immediately after mixing O_3

with C_2H_3CHO. Therefore, HCHO, HCOOH, CO, and CO_2 peaks appear even at 0 min during measurement of FTIR spectra.

Figure 5 shows the dependence of concentrations of O_3 and products on the reaction time in the O_3 + C_2H_3CHO reaction. The C_2H_3CHO concentration slowly decreases exponentially. The concentrations of HCHO and HCOOH increase up to about 0.33 and 1.33 min, respectively, and then decrease thereafter. The CO_2 concentration increases more rapidly than the CO concentration with increasing the reaction time. These results suggest that intermediate HCHO, HCOOH, and CO species are finally converted to CO_2 in the O_3 + C_2H_3CHO reaction.

O_3 molecules are formed through the three-body reactions (6) and (7) and are consumed by photolysis (8) and by the reactions with $O(^3P)$ (9), C_2H_3CHO (10), and other products (11).

$$O + O_2 + N_2 \rightarrow O_3 + N_2 \quad (6)$$
($k_6 = 6.01 \times 10^{-34}$ cm^6 molecule^{-2} s^{-1})[9]

$$O + O_2 + O_2 \rightarrow O_3 + O_2 \quad (7)$$
($k_7 = 6.20 \times 10^{-34}$ cm^6 molecule^{-2} s^{-1})[9]

$$O_3 + h\nu\ (172\text{-nm}) \rightarrow O(^3P,^1D) + O_2 \quad (8)$$

$$O_3 + O(^3P) \rightarrow 2O_2 \quad (9)$$
($k_9 = 1.28 \times 10^{-14}$ cm^3 molecule^{-1} s^{-1})[17]

$$O_3 + C_2H_3CHO \rightarrow \text{products} \quad (10)$$
($k_{10} = 3.63 \times 10^{-19}$ cm^3/molecule^{-1} s^{-1})[17]

$$O_3 + \text{HCHO, HCOOH, CO, and other intermediates} \rightarrow \text{products} \quad (11)$$

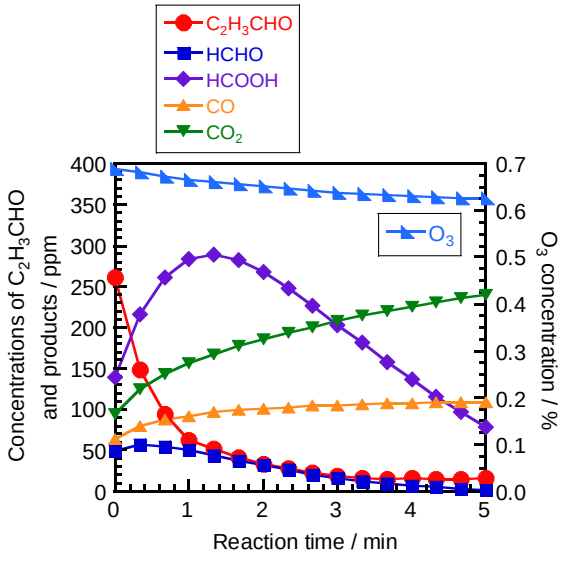

Fig. 5. Dependence of concentrations of C_2H_3CHO, products, and O_3 on the reaction time in air (20% O_2). The initial concentration of O_3 was 260 ppm.

The rate constant of the O_3 + C_2H_3CHO reaction (10) at 298 K is known to be very small. It is smaller than that of the $O(^3P)$ + C_2H_3CHO reaction (2) by a factor of 1.1×10^6 times. Thus it is expected that the contribution of the O_3 + C_2H_3CHO reaction (10) is small under our conditions.

If O_3 molecules are consumed only by the O_3 + C_2H_3CHO reaction (10), little change in the O_3 concentration is expected because of its very small rate constant. However, we found a slow decay of O_3 in the 0–5 min range. Probably ozonides are initially formed by the O_3 + C_2H_3CHO reaction and multiple-step reactions of O_3 with unstable intermediates including ozonides leading to HCOOH, CO, and CO_2 occur. Under such a condition, O_3 is consumed not only by the initial O_3 + C_2H_3CHO reaction but also by many other O_3 + intermediates reactions. Therefore, the apparent removal rate of C_2H_3CHO by O_3 molecules becomes large in comparison with that expected from the rate constant of the O_3 + C_2H_3CHO reaction obtained under single collision conditions.

3.4 Possible decomposition mechanisms of C_2H_3CHO under 172-nm photolysis in air

Scheme 1 shows possible oxidation processes of C_2H_3CHO in air. There are two oxidation mechanisms. One is the direct VUV photolysis (A) and the other is H, $O(^3P,^1D)$, OH, and O_3 reactions (B). The contribution of direct VUV photolysis was estimated using the absorption coefficients at 172-nm for O_2 ($\sigma = 4.63\times10^{-19}$ cm^2/molecule)[15] and for C_2H_3CHO ($\sigma = 1.3\times10^{-17}$ cm^2/molecule[18] and concentrations of O_2 (5–20%) and C_2H_3CHO (500 ppm) from $\sigma_i N_i$ values.[10] Here, σ_i and N_i are absorption cross section of a molecule i, and its number density, respectively. Results show that the contribution of initial absorption of incident light by C_2H_3CHO increases from 6.6% to 12.3 and 21.9% with decreasing the O_2 concentrations from 20% to 10 and 5%, respectively. Therefore, the contribution of direct photolysis by 172-nm VUV photons is not large even at 5% O_2. To the best of our knowledge, there is no information on photolysis products of C_2H_3CHO at 172-nm. Since such products as HCO, CO, and H have been obtained under 193-nm ArF laser photolysis.[19] it is likely that similar products are formed via processes (12a)–(12c) in Scheme 1 under 172-nm photolysis of C_2H_3CHO. It should be noted that active H radicals are formed in process (12c).

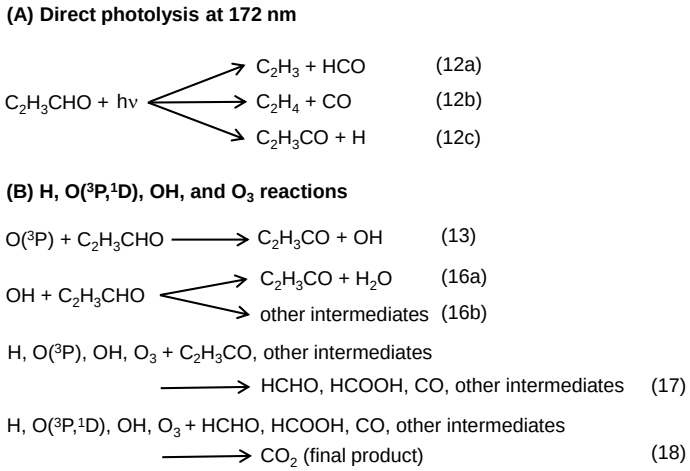

Scheme 1. Possible oxidation processes of acrolein in air.

Major oxidation processes are initiated by the 172-nm photolysis of O_2 into $O(^3P) + O(^1D)$ (1). The contribution of initial absorption of incident light by O_2 was 93.4, 87.7, and 78.1% at O_2 concentrations of 20, 10, and 5%, respectively. After photolysis of O_2, $O(^3P,^1D)$ and O_3 are formed. Results show that the contribution of $O(^1D)$ atoms and O_3 molecules to the C_2H_3CHO removal is small in the initial stage. It is therefore reasonable to assume that the C_2H_3CHO decomposition starts from the $O(^3P) + C_2H_3CHO$ reaction (2). Although no information on products of the $O(^3P) + C_2H_3CHO$ reaction has been reported, it is reasonable to assume that OH radicals are formed though H-abstraction reaction (13) as in the cases of the $O(^3P) + HCHO$ and $O(^3P) + CH_3CHO$ reactions (14) and (15).[10,14]

$$O(^3P) + C_2H_3CHO \rightarrow OH + C_2H_3CO \quad (13)$$

$$O(^3P) + HCHO \rightarrow OH + HCO \quad (14)$$

($k_{14} = 1.67 \times 10^{-13}$ cm^3 molecule^{-1} s^{-1})[17]

$$O(^3P) + CH_3CHO \rightarrow OH + CH_3CO \quad (15)$$

($k_{15} = 4.47 \times 10^{-13}$ cm^3 molecule^{-1} s^{-1})[17]

The rate constant of $OH + C_2H_3CHO$ reaction (16) is larger than that of the $O(^3P) + C_2H_3CHO$ reaction (2) by a factor of 49.[17]

$$OH + C_2H_3CHO \rightarrow \text{Products} \quad (16)$$

($k_{16} = 1.96 \times 10^{-11}$ cm^3 molecule^{-1} s^{-1})[17]

Therefore, it is highly likely that OH radicals play a major role for the C_2H_3CHO removal in our conditions. Further decomposition and oxidation of such intermediates as HCHO, HCOOH, and CO by H, OH, $O(^3P,^1D)$, and O_3 provide CO_2 as a final product. It is known that the $O(^1D) + CO$ reaction leading to CO_2 is fast.

$$O(^1D) + CO \rightarrow CO_2 \quad (19)$$

($k_{19} = 8.00 \times 10^{-11}$ cm^3 molecule^{-1} s^{-1})[17]

Therefore, $O(^1D)$ atom is added as active species in the final step (18) in Scheme 1.

4. Summary and Conclusion

Removal of C_2H_3CHO by a head-on type 172-nm VUV photoirradiation was investigated to develop a photochemical removal technique of VOC at atmospheric pressure and room temperature. At 5–20% O_2 in air, C_2H_3CHO was oxidized to CO_2 via HCHO, HCOOH, and CO. Under 172-nm photolysis of O_2, $O(^3P,^1D)$ and O_3 can be active species for the C_2H_3CHO removal. Results demonstrated that direct photolysis and $O(^3P)$ take part in the initial decomposition of C_2H_3CHO, although the contribution of direct photolysis is less than about 20%. H, $O(^3P,^1D)$, OH, and O_3 contribute to the further oxidation of such intermediates as HCHO, HCOOH and CO leading to a final product CO_2. The highest initial removal rate of C_2H_3CHO in air, 1.43 min^{-1}, was obtained at a low O_2 concentration of 5%. These findings provide fundamental data required for the development of practical removal apparatus of C_2H_3CHO using a head-on type of 172-nm VUV lamp in air at atmospheric pressure.

Acknowledgments

This work was supported by NEDO (project number NCJJ200049, 2008−2009,), and City Area Project from Fukuoka Prefecture (2009).

References

1) Q. Hong, S. Dezhi, and C. Guoqing, *J. Environ. Sci.*, 19, excimer lamp at atmospheric pressure 1136 (2007).
2) L. Yang, Z. Liu, J. Shi, Y. Zhang, H. Hu, and W. Shangguan, *Sep. Purif. Techonol.*, 54, 204 (2007).
3) P. Fu, P. Zhanga, and J. Li, *Appl. Catal. B Environ.*, 105, 220 (2011).
4) M. Y. Wang, Y. W. Lu, F. Wu, X. J. Zhang, and C. X. Yang, *Procedia Eng.*, 121, 521 (2015).
5) Z. Zhang, Z. Jiang, W. Shangguan, *Catal. Today*, 264, 270 (2016).
6) S. Cheng, Y. Li, C. Yuan, P. Tsai, H. Shen, and C. Hung, *Aerosol and Air Quality Research*, 18, 3220 (2018).
7) B. Robert and G. Nallathambi, *Environ. Chem. Lett.*, 19, 2551 (2021).
8) M. Tsuji, T. Kawahara, N. Kamo, and M. Miyano, *Bull. Chem. Soc. Jpn.*, 83, 582 (2010).
9) M. Tsuji, T. Kawahara, K. Uto, N. Kamo, M. Miyano, J. Hayashi, and T. Tsuji, *Environ. Sci. Pollut. Res.*, 25, 18980 (2018).
10) M. Tsuji, M. Miyano, N. Kamo, T. Kawahara, K. Uto, J. Hayashi, and T. Tsuji, *Environ. Sci. Pollut. Res.*, 26, 11314 (2019).
11) M. Tsuji, M. Miyano, N. Kamo, T. Kawahara, K. Uto, J. Hayashi, and T. Tsuji, *Int. J. Environ. Sci. Technol.*, 16, 7229 (2019).
12) M. Tsuji, N. Kamo, M. Miyano, and M. Kawahara, *Engineering Sciences Reports, Kyushu University*, 46, 19 (2024).
13) M. Tsuji, N. Kamo, and M. Miyano, *Engineering Sciences Reports, Kyushu University*, 47, 1 (2025).
14) M. Tsuji and M. Miyano, *Engineering Sciences Reports, Kyushu University*, 47, 9 (2025).
15) H. Okabe, "*Photochemisty of Small Molecules*", John Wiley & Sons, New York (1978).
16) J. B. Nee, P. C. Lee, *J. Phys. Chem. A*, 101, 6653 (1997).
17) *NIST Chemical Kinetics Database on the Web, Standard Reference Database 17, Version 7.1 (Web Version)*, Release 1.6.8, Data Version 2025. http://kinetics.nist.gov/kinetics/index.jsp.
18) O. Geßner, E. t.-H. Chrysostom, A. M. D. Lee, D. M. Wardlaw, M.-L. Ho, S.-J. Lee, B.-M. Cheng, M. Z. Zgierski, I.-C. Chen, J. P. Shaffer, C. C. Hayden, and A. Stolow, *Faraday Discuss.*, 127, 193 (2004).
19) C. Chaudhuri and S. H. Lee, *Phys. Chem. Chem. Phys.*, 13, 7312 (2011).